

Role of charge transfer in catalytic hydrogen oxidation over platinum

Sergey N. Maximoff^{1, 2, a)}

¹⁾*Department of Chemistry, University of California, Berkeley,
USA*

²⁾*Department of Chemistry and Biochemistry, Loyola University, Chicago, IL,
USA*

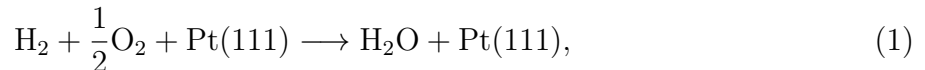
Charge transfer plays the central role in chemisorption and chemical reactions at metal surfaces. The Somorjai group in *Nano. Lett.* **9**, 3930 (2009) has reported a chemicurrent, a flux of charge carriers in response to H₂ oxidation by O₂ into H₂O over a platinum surface. The nature of the chemicurrent has been debated in the literature; explanations both extrinsic and intrinsic to the reaction mechanism have been offered. This article suggests a picture behind the chemicurrent experiments, which is intrinsic to the mechanism of hydrogen oxidation in a high temperature regime. Surface reaction intermediates, “O⁻”, “H⁻”, “OH⁻”, are negatively charged while the product, H₂O, and reactants, H₂ and O₂, are neutral. Hence, charge transfers between the metal and reacting species are inevitable. After electrons are transferred from the metal to the interface in dissociative oxygen and hydrogen adsorption, translationally excited electrons in the metal arise in part as a result of decay of negatively charged transition states in reaction steps connecting surface species of different charges, “O⁻ + H⁻” \rightleftharpoons “2e + OH⁻” and “OH⁻ + H⁻” \rightleftharpoons “2e + H₂O”. These transition states are the lowest energy configurations possible for changing the charge of the negatively charged surface intermediates. In particular, the transition state for “O⁻ + H⁻” \rightleftharpoons “2e + OH⁻” limits the reaction rate. These processes may contribute to the chemicurrent. This picture should also apply to other catalytic chemical reactions on metal surfaces that proceed through formation of charged surface intermediates and their consequent discharge into the metal.

^{a)}To whom correspondence should be addressed: SNMaximoff@gmail.com

I. INTRODUCTION

Absorption of light in metals may produce hot internal electrons whose kinetic energies exceed typical thermal values¹. Exothermic chemistry at low workfunction metal surface may eject electrons from metal in the form of exoelectrons^{2,3}. Evidence has been mounting^{3–13} that exothermic redox chemical reactions at high workfunction surfaces of electron-rich noble and late transition metals may also invoke hot electron excitations that propagate for about a few nanometers into the metal at kinetic energies $\gtrsim 0.5–1.2$ eV, but below the workfunction barrier for electron ejection from the metal (4.3–5.9 eV¹⁴). These excitations must propagate inside the metal rather than in a vacuum, and therefore are tricky to probe directly in experiments. Methods of their detection are based on Schottky diode experiments (figs. 1(a) and 1(b)). These experiments aim to register these excitations indirectly as a zero voltage bias electric current through high workfunction metal film/semiconductor Schottky diodes with 0.5–1.2 eV Schottky barriers^{4,8,15} during adsorption-desorption or reactive adsorption-desorption of molecules or atoms at the interface between the gas and the diode at pressures ranging from ultra high vacuum (UHV) to pressures on the order of one bar⁴. A catalytic Schottky diode is a thin film of a catalytic metal that joins a thicker film of a semiconductor so that the Schottky barrier at the interface of the metal and semiconductor passes the current of thermal electrons in the direction from the semiconductor to the metal but not in the opposite direction. However, a current originating at the surface and passing through the metal film may circumvent the Schottky barrier and enter the semiconductor when the kinetic energy of carriers exceeds the Schottky barrier height. These hot carriers, which a surface chemical reaction may generate, would then contribute to the zero bias current through the diode.

The Refs. 4 and 16 have reported that an exothermic catalytic chemical process (the reaction heat of -2.51 eV per an H_2O ¹⁷) at the constant partial pressures $p_{\text{H}_2} = 6$ Torr and $p_{\text{O}_2} = 760$ Torr,



over a 5 nm thick Pt film in Pt/n-TiO₂ diode with the Schottky barrier of 1.1–1.2 eV induces a zero-bias current. Refs. 4 and 16 further separate this current into a component due to a temperature gradient across the Schottky diode (thermoelectric current) and another component proportional to the reaction rate — the chemicurrent. This partitioning scheme does

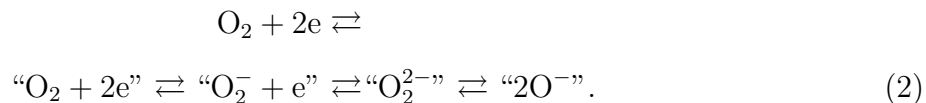
not expose molecular mechanisms, which are responsible for the measured zero-bias current, and it has been debated in the literature^{10,18,19} whether chemicurrent is a phenomenon that has to do with charge transfer surface chemistry at high pressure conditions.

It is not at all new that internal degrees of freedom of molecules play a role in energy flow between metal electrons and molecules through transient retention of metal electrons by the internal degrees of freedom^{20,21}. Refs. 7 and 22 bring up the significance of temporary molecular anions in energy relaxation in molecular scattering against metal surfaces. Refs. 23–25 discuss how transient charge transfer between adsorbates and metal surfaces facilitates rovibrational energy relaxation. A review²⁶ discusses exoelectron emission during oxygen adsorption on alkali metal surfaces. It can happen in chemical reactions that the number of electrons localized at reacting intermediates changes significantly and rapidly upon crossing the activation barrier at a transition state (i.e., a saddle point at the ground state adiabatic surface) along the reaction coordinate²⁷. This structure of the ground state adiabatic surface conveys an instability in the number of electrons localized at the interface in the adiabatic ground state and preconditions non-adiabatic conversion of high internal energy at the transition state into kinetic energy of delocalized metal electrons. As it turns out, this latter picture is relevant in the catalytic hydrogen oxidation reaction eq. (1).

This article examines eq. (1) in a particular case of a high temperature regime when water is not present at the Pt(111) interface to reveal typical events that may contribute to the chemicurrent. In this case, the reaction mechanism is relatively well-understood²⁸. In particular, it can be scrutinized theoretically for potential sources of chemicurrent. First, O₂ and H₂ from the gas dissociatively adsorb at the interface and give rise to chemisorbed O²⁹ and H³⁰. Second, a surface hydroxyl, OH, forms. Third, a water molecule forms upon hydrogenation of OH.

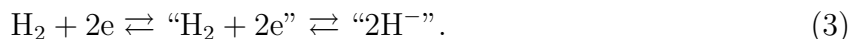
The dissociative O₂ adsorption on Pt(111) (heat of dissociative adsorption is -2.0 eV per an O₂ at the saturation coverage) is a sequential electron attachment process. O₂ remains physisorbed and uncharged, “O₂” (quotation marks enclose an interfacial specie), at $T \lesssim 45$ K^{31–34}, it converts to the charged superoxide, “O₂⁻”, in the temperature range 90 – 135 K^{35,36}, and then to the charged peroxide, “O₂²⁻”, in the temperature range 135 –

150 K³¹⁻³³, and then to the pair of oxygen ions, “O⁻ + O⁻”, at higher temperatures,

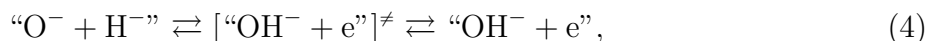


The observed increase in the electronic workfunction of Pt(111) upon adsorption¹⁴, core level spectroscopies^{32,33}, the O–O bond elongation, and electronic structure calculations³⁷ all indicate that the negative charge progressively increases from virtually none in “O₂”, to larger values in “O₂⁻” and in “O⁻”, due to charge transfer from the metal to interfacial electronic states derived from the lowest unoccupied molecular orbitals (LUMO) of O₂.

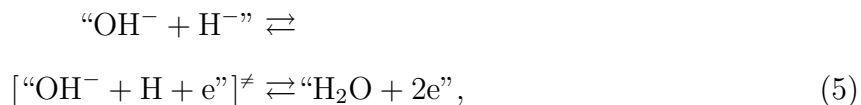
The Pt(111) interface must be predominantly covered with oxygen in the excess oxygen⁴. Therefore, H₂ dissociates on Pt(111) precovered with O (initial heat of adsorption is around -0.7 eV per an H₂). Dissociative H₂ adsorption^{14,30} on most metal surfaces results in a charge transfer from the metal that causes formation of “H⁻”,



If “H₂O” is not present at the interface, the reaction proceeds through



at a relatively high activation energy of 0.69 eV³⁸. An “OH⁻” in eq. (5) further recombines with a “H⁻”,



at an activation energy lower than that for “OH⁻” formation³⁹⁻⁴¹.

The product, H₂O in eq. (5), and the reactants, H₂ and O₂ in eqs. (2) and (3), are electroneutral, but the above discussion indicates that eq. (1) involves anionic intermediates at the metal-gas interface. Since the chemical process in eq. (1) is catalytic, the anionic intermediates are not permanent, and, by charge conservation, an intermittent charge flux from and to the interface is inevitable. In what follows, this article relies on quantum chemistry models to show that eq. (1) necessitates intermittent charge transfers from the interface to metal. These charge transfers occur at high energy configurations that correlate with the transition states [“OH⁻ + H + e”][‡] and [“OH⁻ + e”][‡]. The barriers at these transition states

are the activation barriers for associative electron detachment events. For the associative electron detachment events to proceed, the total energy of the colliding anionic intermediates on the left-hand sides of eq. (5) must exceed the minimum barrier for electron detachment into the conduction band of the metal from the interface (the middle terms in eq. (4) and eq. (5)).

II. METHODS

The Pt(111) metal-vacuum interface is modeled by 4 layer hexagonal $p(2n \times 2m)$ -Pt slabs with $n, m = 1, 2$ with a single side open for adsorption. The spacing between the periodically replicated parallel slabs in the direction perpendicular to the surface is maintained above 17 Å to diminish the spurious dipole-dipole interaction between the slabs that asymptotically decreases as the inverse cube of the separation distance. A long-range ordered honeycomb $p(2 \times 2) - \text{O}$ pattern in register with Pt(111) such that every other *fcc* site is occupied by “O⁻”⁴² corresponds to the 0.25 monolayer of “O⁻” saturation coverage upon exposure of Pt(111) to O₂ at $T \gtrsim 150$ K. This structure is taken as a model of oxygen adsorption.

Numerical density functional theory calculations with periodic boundary conditions in this work have been done using the Quantum-ESPRESSO suite of computer programs⁴³. The exchange-correlation energy is given by the PW91 generalized gradient approximation⁴⁴. The core electrons in H, [He] O, [Xe] Pt are described by ultrasoft pseudopotentials, which are fitted to reproduce the numerical Kohn-Sham orbitals of the atoms⁴³. The ultrasoft pseudopotential for Pt includes the scalar relativistic effects as well as the non-linear core corrections. The Kohn-Sham orbitals and the charge density of the valence electrons are expanded into the Fourier series over plane waves with kinetic energies below 612.26 eV and 6122.6 eV, respectively.

The equilibrium geometries are computed by variable cell relaxation runs until the total force and the stress falls below 0.026 eV/Å and 1 kbar, respectively. Minimum energy pathways connecting the equilibrium structures on the adiabatic ground state surface are sampled by the nudged elastic bands (NEB) method⁴⁵. A string of intermediate structures interpolating between the initial and final equilibrium structures is varied until forces perpendicular to the path fall below 0.094 eV/Å. In the NEB and geometry optimization calculations, the integrals over the irreducible surface Brillouin zone of the hexagonal $p(2n \times 2m)$ lattice are

discretized over $4/n \times 4/m$ Monkhorst-Pack grid⁴⁶ with the Methfessel-Paxton first-order smearing⁴⁷ of 0.204 eV.

The electronic structure at fixed configurations of atomic cores is quantified by projected densities of states and by Bader atomic charges⁴⁸. The reciprocal space integrals in the expressions for the density of electronic states, the electron number density, and the Fermi level are computed over $32/n \times 32/n$ Monkhorst-Packs grid using the tetrahedron method⁴⁹. The projected density of states is computed using projections on the valence atomic orbitals.

III. RESULTS AND DISCUSSION

Figure 2 shows the density of the electronic states at “O⁻” in the saturation coverage structure, $p(2 \times 2)$ -O_{fcc} (fig. 3(a)). The excesses of electrons at the $2p_{\text{O}}$ orbitals and the depletion of electrons at the $5d$ orbitals are readily seen within the triangle of the interfacial Pt sites surrounding the fcc hollow sites in the interfacial layer, as well as in the d_{z^2} orbital of the Pt atom just beneath the fcc hollow site. These observations are consistent with the picture of O₂ adsorption, which is established in the literature^{50,51}.

Figure 2 shows the density of the electronic states at “H⁻”. The bonding $1s_{\text{H}}$ -metal states are below the Fermi level. The excess electron density in fig. 3(a) indicates the excess of electrons at the $1s_{\text{H}}$ orbitals of “H⁻” and the deficit of the electrons at the Pt $5d6s$ orbitals underneath. The charge of an oxygen atom in $p(2 \times 2)$ -O_{fcc} (fig. 3(a)) is 0.75 e. The charges of oxygen and hydrogen atoms in $p(2 \times 2)$ -O_{fcc} + H_{top} coadsorption structure are 0.75 and 0.02 e, respectively.

As figs. 3(a,b) show, the co-adsorbed “O⁻” and “H⁻” must overcome an activation barrier, $\chi_{\text{OH(l)}}^{\ddagger} = 0.79$ eV, during the up-hill step P'_2 , before “OH⁻” forms during the down-hill step P''_2 . As fig. 4(a) indicates, the excess electron density in fig. 3(a) transforms from the initial $1s_{\text{H}}$ - and $2p_{\text{O}}$ -like distribution to a bond-centered distribution during $P''_{\text{OH(l)}}$, a fraction of the electrons redistributes to the non-bonding $1\pi_{\text{OH}}$, where they remain, while the rest return to the metal. The latter is indicated by the drop in the charge at the adsorbates by 0.17 e during P'_2 and then by 0.24 e during P''_2 (fig. 3(c)). With the charge now concentrated at the non-bonding lone pairs $1\pi_{\text{OH}}$, “OH⁻” assumes the O-end down position (fig. 3(a)). The energy that these electrons may take is estimated by the energy drop, $\delta u_{\text{OH(l)}} = 1.1$ eV, during P''_2 .

As fig. 3(a) shows, “H⁻” from an *fcc* hollow site migrates to a bridge site adjacent to the atop “OH⁻” during P_4'' , and then moves towards the “OH⁻” along the asymmetric stretch of the nascent water molecule during P_4' . The energy in fig. 3(b) increases towards the activation barrier, $\chi_{\text{H}_2\text{O}}^\ddagger = 0.3$ eV, at $\text{H}_2\text{O}^\ddagger$ during P_4' . It drops by $\delta u_{\text{H}_2\text{O}}^\ddagger$ (about 1.2 eV) to the minimum at “H₂O” during P_4'' . Meanwhile, the charge in fig. 3(c) increases by 0.1 e during P_4' , and then increases by 0.94 eV during P_4'' , indicating charge transfer to the metal. This behavior is caused by the emptying of the continuum of the H \cdots OH LUMO ($4a_1$)-derived states that host the excess charge before the transition configuration, $\text{H}_2\text{O}^\ddagger$ as fig. 4(b) illustrates. In other words, $\text{H}_2\text{O}^\ddagger$ is an “H \cdots OH⁻” that is just about to desorb while simultaneously autoionizing into the metal conduction band.

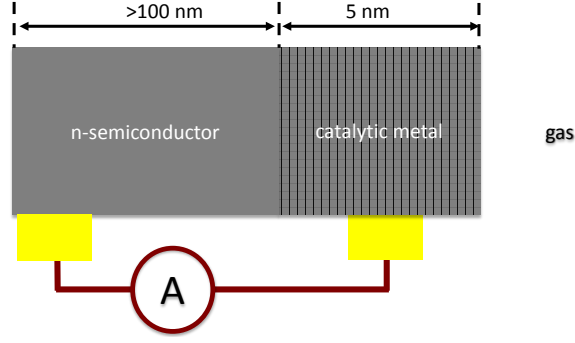
Electron transfers in surface chemical events eqs. (2) to (5) define a surface electron pump, which may contribute to the chemi-current during catalytic hydrogen oxidation eq. (1) on Pt(111) in a high temperature regime when water does not remain at the interface. The legs that form a cycle of the pump are consequent reduction and oxidation reaction. Delocalized conduction electrons from the metal localize at the interface along the reductive legs when surface anions form (i.e., in dissociative adsorption of hydrogen eq. (3) and oxygen eq. (2)). Then these localized electrons return to the metal during the oxidative leg of the cycle when the surface anions autoionize (i.e., in the formation of hydroxyl eq. (4) and water eq. (5)). It has long been established that metal electron can be excited in exothermic oxygen adsorption over metal surfaces²⁶. Some of the heat released in this reaction is likely to excite metal electrons here. Charge transfers from the interface to the metal during the oxidative steps take place at transition states, which are high in energy compared to the final states (1.1 – 1.2 eV). Upon relaxation towards the final state, this excess energy must be shared between the rovibrational and electronic degrees of freedom, and, in the latter case, may channel to the chemi-current in a Schottky diode with a low enough barrier. A possible energy transfer scenario involves $4a_1$ -derived states of a nascent water molecule, which carry electrons localized at or before the anionic transition state to delocalized metal conduction electrons above the Fermi level at the electroneutral product water molecule. This picture is reminiscent to that seen in the context of catalytic CO oxidation on Pt(111)²⁷, which also exhibits chemi-current^{52,53} and involves charge transfer transition states. Mechanism of eq. (1) at low temperature when water is present at the surface is considerably more involved^{39,40,54}. However, hydrated anions must develop in this reaction, and these anions

must change their charges during reaction steps (e.g., “ $(\text{H}_2\text{O})_{n+1}\text{O}^- + e^- \rightleftharpoons (\text{H}_2\text{O})_n(\text{OH})_2^{2-}$ ” and “ $(\text{H}_2\text{O})_n(\text{OH})_2^{2-} + \text{H}^- \rightleftharpoons (\text{H}_2\text{O})_{n+1}(\text{OH})^- + 2e^-$ ”). These changes would occur at transition states just as in CO oxidation and hydrogen oxidation at high temperature.

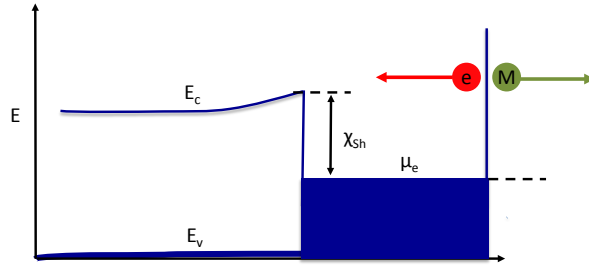
This article does not make any specific determination about the energy that these electrons carry; a model beyond the adiabatic limit would be required to make such a determination and will be discussed elsewhere. However, the conclusion about the existence and importance of the charge transfer transition states in hydrogen oxidation, as those configurations where the adiabatic picture fails in a particular way, follows already from the structure of the ground state adiabatic potential.

ACKNOWLEDGMENTS

The author thanks L.R. Backer, Y. Borodko, A. Hervier, J.R. Renzas G.A. Somorjai, J.Y. Park for comprehensive and stimulating discussions on the subject of their experimental work. The author also thanks M. Head-Gordon for multiple stimulating discussions and providing critical comments on the manuscript. This work was supported by the U.S. Department of Energy, Office of Basic Energy Sciences, Chemical Sciences, Geosciences, and Biosciences Division, through Contract No. DEAC02-05CH11231. This work used resources of the National Energy Research Scientific Computing Center.



(a)



(b)

FIG. 1. (a) The Schottky diode. The chemistry takes place at the interface of the gas and the catalytic metal (right), the catalytic metal joins the n -semiconductor over the Schottky contact. The Ohmic contacts (the yellow bars) collect the charge from the catalytic metal and the semiconductor. The wires (brown lines) close the circuit through the ammeter. (b) An energy diagram of the Schottky diode. The chemical potential of the electrons (μ_e) is below the Schottky barrier (χ_{sh}). If a chemical process excites a charge whose kinetic energy at the Schottky contact exceeds the Schottky barrier, the charge enters the semiconductor where it travels in the conduction band (E_c) above the valence band (E_v). The workfunction and the absorption barriers (the rightmost blue vertical line) prevent the electrons from spilling into the gas and the molecular species from entering the metal, respectively.

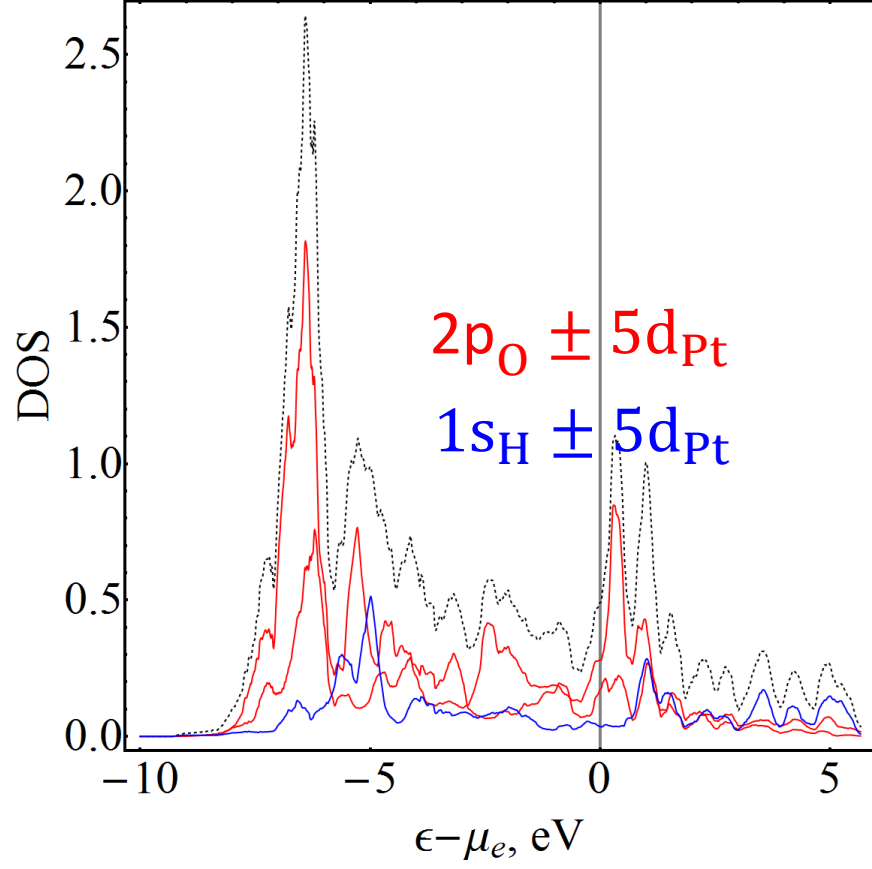


FIG. 2. The density of the Kohn-Sham electronic states at the coadsorbed O and H ions (the black curve), that of the $2p_{O\parallel} \pm 5d_{Pt}$ states (the upper red curves), the $2p_{O\perp} \pm 5d_{Pt}$ states (the upper red curves), that of the $1s_H \pm 5d_{Pt}$ states (the blue curve).

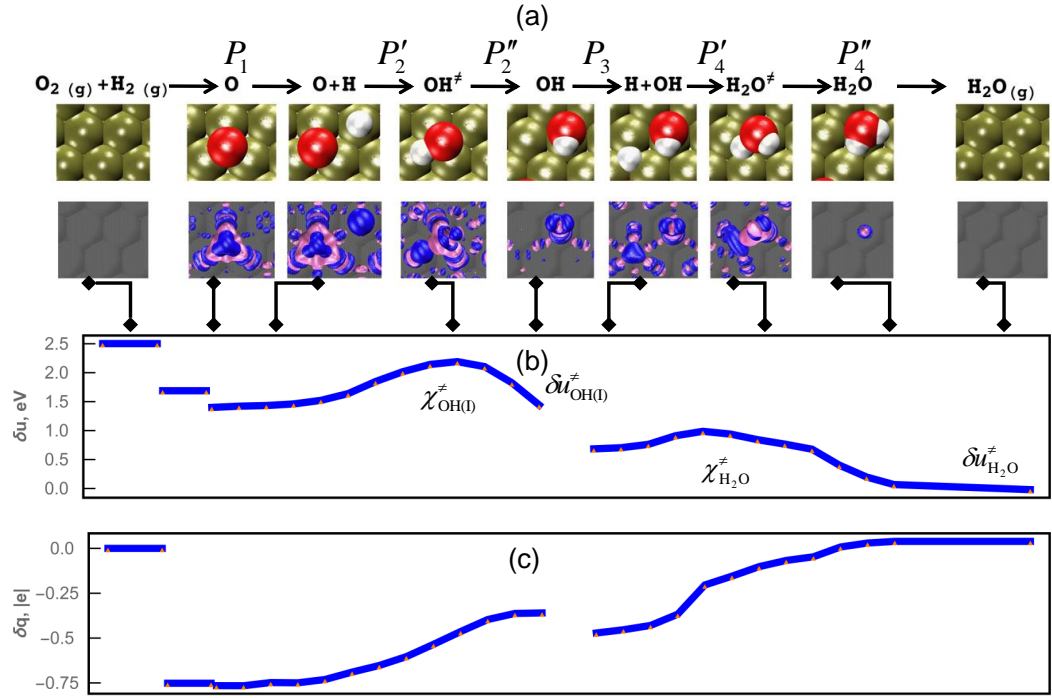


FIG. 3. Along minimum energy reaction paths are shown: (a) the surface oxygen (red balls) and hydrogen (white balls) atoms on Pt(111) (upper row), and the surface electron density ± 0.005 contour values relative to that decoupled from the metal adsorbate layer and that of Pt(111) (blue and pink represent build up and depletion of electrons, respectively); (b) the changes in the energy with respect to the clean Pt(111) slab and a free H_2O ; (c) the charge at the interface.

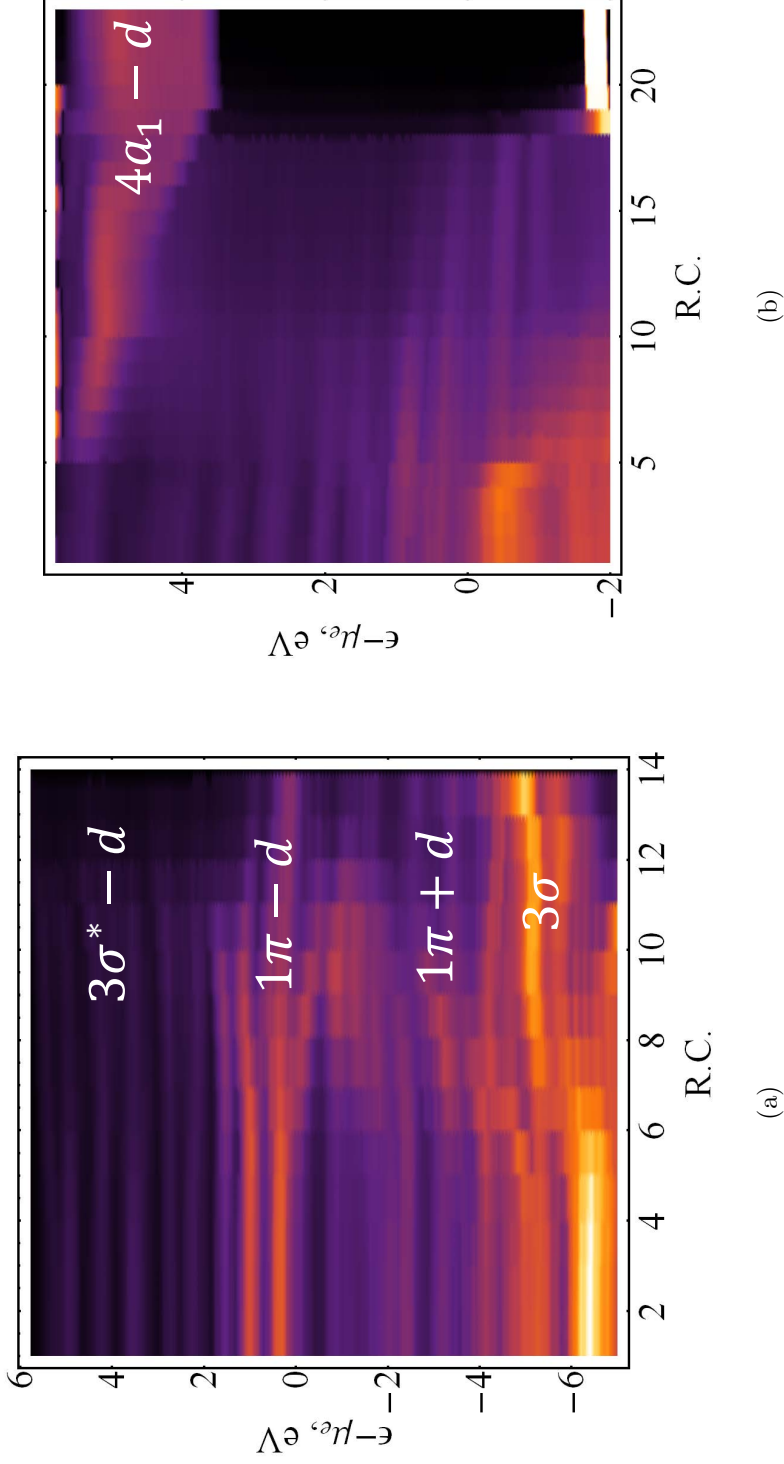


FIG. 4. The density of the Kohn-Sham electronic states along (a) the segment of the reaction path describing the event “ $\text{O}^- + \text{H}^- \rightarrow \text{OH}^- + \text{e}^-$ ”, and (b) along the segment P_4 of the reaction path describing the event “ $\text{OH}^- + \text{H}^- \rightarrow \text{H}_2\text{O} + 2\text{e}^-$ ”. The vertical axis is the Kohn-Sham binding energy with respect to the Fermi level. The horizontal axis is the reaction coordinate. The brighter and darker colors correspond to higher and lower values of the density of states, respectively. In (a), σ_{OH} and σ_{OH}^* and $1\pi_{\text{OH}}$ hybridize with the platinum 5d6s bands at the interface to give rise to the split bonding and antibonding bands. In (b), the $4a_1 - d$ -derived unoccupied delocalized states can carry the electrons that previously resided within the occupied surface states.

REFERENCES

- ¹H. Petek and S. Ogawa, *Progress in Surface Science* **56**, 239 (1997).
- ²A. Böttcher, R. Imbeck, A. Morgante, and G. Ertl, *Phys. Rev. Lett.* **65**, 2035 (1990).
- ³H. Nienhaus, *Surf. Sci. Rep.* **45**, 1 (2002).
- ⁴A. Hervier, J. R. Renzas, J. Y. Park, and G. A. Somorjai, *Nano Lett.* **9**, 3930 (2009).
- ⁵K. Schierbaum and M. El Achhab, *Phys. Status Solidi A* **208**, 2796 (2011).
- ⁶Y. Huang, C. T. Rettner, D. J. Auerbach, and A. M. Wodtke, *Science* **290**, 111 (2000).
- ⁷N. Shenvi, S. Roy, and J. C. Tully, *Science* **326**, 829 (2009).
- ⁸B. Gergen, H. Nienhaus, W. H. Weinberg, and E. W. McFarland, *Science* **294**, 2521 (2001).
- ⁹J. R. Renzas and G. A. Somorjai, *J. Phys. Chem. C* **114**, 17660 (2010).
- ¹⁰M. A. Hashemian, S. K. Dasari, and E. G. Karpov, *J. Vac. Sci. Technol. A* **31**, 020603 (2013).
- ¹¹B. Schindler, D. Diesing, and E. Hasselbrink, *J. Phys. Chem. C* **117**, 6337 (2013).
- ¹²H. Nienhaus, H. S. Bergh, B. Gergen, A. Majumdar, W. H. Weinberg, and E. W. McFarland, *Phys. Rev. Lett.* **82**, 446 (1999).
- ¹³J. Y. Park, L. R. Baker, and G. A. Somorjai, *Chemical Reviews* **115**, 2781 (2015), PMID: 25791926, <http://dx.doi.org/10.1021/cr400311p>.
- ¹⁴K. Jacobi, ed., *Electron work function of metals and semiconductors*, Landolt-Brnstein - Group III Condensed Matter, Vol. 42A2 (Springer-Verlag, 2005).
- ¹⁵A. M. Wodtke, D. Matsiev, and D. J. Auerbach, *Prog. Surf. Sci.* **83**, 167 (2008).
- ¹⁶H. Lee, I. I. Nedrygailov, C. Lee, G. A. Somorjai, and J. Y. Park, *Angewandte Chemie International Edition* **54**, 2340 (2015).
- ¹⁷P. J. Linstrom and W. G. Mallard, eds., *NIST Chemistry WebBook, NIST Standard Reference Database Number 69* (National Institute of Standards and Technology, Gaithersburg MD, 20899, 2013).
- ¹⁸J. R. Creighton and M. E. Coltrin, *The Journal of Physical Chemistry C* **116**, 1139 (2012), <http://dx.doi.org/10.1021/jp210492k>.
- ¹⁹I. I. Nedrygailov, E. G. Karpov, E. Hasselbrink, and D. Diesing, *Journal of Vacuum Science & Technology A: Vacuum, Surfaces, and Films* **31**, 021101 (2013).
- ²⁰J. C. Tully, *Ann. Rev. Phys. Chem.* **51**, 153 (2000).

- ²¹D. J. Auerbach and A. M. Wodtke, *Dynamics of Gas-Surface Interactions*, edited by R. Dez Muio and H. F. Busnengo, Springer Series in Surface Sciences, Vol. 50 (Springer Berlin Heidelberg, 2013) pp. 267–297.
- ²²J. W. Gadzuk, *J. Chem. Phys.* **79**, 6341 (1983).
- ²³M. Persson and B. Hellsing, *Phys. Rev. Lett.* **49**, 662 (1982).
- ²⁴M. Head-Gordon and J. C. Tully, *J. Chem. Phys.* **103**, 10137 (1995).
- ²⁵V. Krishna and J. C. Tully, *J. Chem. Phys.* **125**, 054706 (2006).
- ²⁶T. GREBER, A. MORGANTE, S. FICHTNER-ENDRUSCHAT, and G. ERTL, *Surface Review and Letters* **02**, 273 (1995), <http://www.worldscientific.com/doi/pdf/10.1142/S0218625X95000285>.
- ²⁷S. N. Maximoff and M. P. Head-Gordon, *Proc. Nat. Acad. Sci.* **106**, 11460 (2009).
- ²⁸G. A. Somorjai and Y. Li, *Introduction to Surface Chemistry And Catalysis* (Wiley, 2010).
- ²⁹J. L. Gland, B. A. Sexton, and G. B. Fisher, *Surf. Sci.* **95**, 587 (1980).
- ³⁰J. Ludwig and D. G. Vlachos, *J. Chem. Phys.* **128**, 154708 (2008).
- ³¹A. C. Luntz, J. Grimblot, and D. E. Fowler, *Physical Review B* **39**, 12903 (1989).
- ³²W. Wurth, J. Stöhr, P. Feulner, X. Pan, K. R. Bauchspiess, Y. Baba, E. Hudel, G. Rocker, and D. Menzel, *Physical Review Letters* **65**, 2426 (1990).
- ³³C. Puglia, A. Nilsson, B. Hernnäs, O. Karis, P. Bennich, and N. Martensson, *Surf. Sci.* **342**, 119 (1995).
- ³⁴A. N. Artsyukhovich, V. A. Ukraintsev, and I. Harrison, *Surf. Sci.* **347**, 303 (1996).
- ³⁵H. Steininger, S. Lehwald, and H. Ibach, *Surf. Sci.* **123**, 1 (1982).
- ³⁶J. Yoshinobu and M. Kawai, *J. Chem. Phys.* **103**, 3220 (1995).
- ³⁷A. Eichler and J. Hafner, *Physical Review Letters* **79**, 4481 (1997).
- ³⁸A. Anton and D. C. Cadogan, *Surf. Sci.* **239**, L548 (1990).
- ³⁹S. Völkening, K. Bedürftig, K. Jacobi, J. Wintterlin, and G. Ertl, *Phys. Rev. Lett.* **83**, 2672 (1999).
- ⁴⁰A. Michaelides and P. Hu, *J. Am. Chem. Soc.* **123**, 4235 (2001).
- ⁴¹G. S. Karlberg, G. Wahnstrom, C. Clay, G. Zimbitas, and A. Hodgson, *J. Chem. Phys.* **124**, 204712 (2006).
- ⁴²N. Materer, U. Starke, A. Barbieri, R. Dll, K. Heinz, M. V. Hove, and G. A. Somorjai, *Surf. Sci.* **325**, 207 (1995).

- ⁴³P. Giannozzi, S. Baroni, N. Bonini, M. Calandra, R. Car, C. Cavazzoni, D. Ceresoli, G. L. Chiarotti, M. Cococcioni, I. Dabo, A. Dal Corso, S. de Gironcoli, S. Fabris, G. Fratesi, R. Gebauer, U. Gerstmann, C. Gougoussis, A. Kokalj, M. Lazzeri, L. Martin-Samos, N. Marzari, F. Mauri, R. Mazzarello, S. Paolini, A. Pasquarello, L. Paulatto, C. Sbraccia, S. Scandolo, G. Sclauzero, A. P. Seitsonen, A. Smogunov, P. Umari, and R. M. Wentzcovitch, *J. Phys. Condens. Matter* **21**, 395502 (19pp) (2009).
- ⁴⁴J. P. Perdew, J. A. Chevary, S. H. Vosko, K. A. Jackson, M. R. Pederson, D. J. Singh, and C. Fiolhais, *Phys. Rev. B* **46**, 6671 (1992).
- ⁴⁵G. Mills, H. Jonsson, and G. K. Schenter, *Surf. Sci.* **324**, 305 (1995).
- ⁴⁶H. J. Monkhorst and J. D. Pack, *Phys. Rev. B* **13**, 5188 (1976).
- ⁴⁷M. Methfessel and A. T. Paxton, *Phys. Rev. B* **40**, 3616 (1989).
- ⁴⁸G. Henkelman, A. Arnaldsson, and H. Jansson, *Comput. Mater. Sci.* **36**, 354 (2006).
- ⁴⁹P. E. Blöchl, O. Jepsen, and O. K. Andersen, *Phys. Rev. B* **49**, 16223 (1994).
- ⁵⁰I. Panas and P. Siegbahn, *Chem. Phys. Lett.* **153**, 458 (1988).
- ⁵¹*Landolt-Börnstein's Numerical Data and Functional Relationships in Science and Technology*, Group III Condensed Matter (Springer-Verlag, 2005).
- ⁵²X. Ji, A. Zupperro, J. M. Gidwani, and G. A. Somorjai, *Nano Lett.* **5**, 753 (2005).
- ⁵³X. Z. Ji and G. A. Somorjai, *J. Phys. Chem. B* **109**, 22530 (2005).
- ⁵⁴G. B. Fisher and B. A. Sexton, *Phys. Rev. Lett.* **44**, 683 (1980).